ELSEVIER

Physica D 111 (1998) 243–264

PHYSICA D

Turbulent binary fluids: A shell model study

Mogens H. Jensen *, Poul Olesen [1]

The Niels Bohr Institute, University of Copenhagen Blegdamsvej 17, DK-2100 Copenhagen, Denmark

Received 11 February 1997; received in revised form 23 May 1997; accepted 4 June 1997
Communicated by U. Frisch

Abstract

We introduce a shell ("GOY") model for turbulent binary fluids. The variation in the concentration between the two fluids acts as an active scalar leading to a redefined conservation law for the energy, which is incorporated into the model together with a conservation law for the scalar. The model is studied numerically at very high values of the Prandtl and Reynolds numbers and we investigate the properties close to the critical point of the miscibility gap where the diffusivity vanishes. A peak develops in the spectrum of the scalar, showing that a strongly turbulent flow leads to an increase in the mixing time. The peak is, however, not very pronounced. The mixing time diverges with the Prandtl number as a power law with an exponent ≈ 0.9. The continuum limit of the shell equations leads to a set of equations which can be solved by a scaling ansatz, consistent with an exact scaling of the Navier–Stokes equations in the inertial range. In this case a weak peak also persists for a certain time in the spectrum of the scalar. Exact analytic solutions of the continuous shell equations are derived in the inertial range. Starting with fluids at rest, from an initial variation of the concentration difference, one can provoke a "spontaneous" generation of a velocity field, analogous to MHD in the early universe.

Keywords: Binary fluids; Turbulence; Shell models; Intermittency; Continuum limit

1. Introduction: Turbulent fluid mixtures

Binary fluid mixtures provide a beautiful example of physical systems where it is possible to study the behavior in the limit of exceedingly large values of the Prandtl number. This is the case for miscible binary mixtures just above the consolute temperature T_c, at which the diffusivity vanishes as a power law (for a review, see [1])

$$D(T) \simeq D_0 \left(\frac{T - T_c}{T_c} \right)^{\mu} \tag{1}$$

with an exponent in the range

$$\mu \sim 0.63 - 0.74. \tag{2}$$

* Corresponding author. E-mail: mhjensen@nbi.dk.
[1] E-mail: polesen@nbi.dk.

PII S0167-2789(97)00138-3

Since $D(T) \to 0$ at the critical point, the corresponding Prandtl number $Pr = \nu/D \to \infty$ and values as high as 10^6 can be obtained experimentally [1]. Goldburg and coworkers [2–5] studied turbulent binary mixtures experimentally using light scattering techniques. One can measure both the variation of the mixing times and the growth of domains using these techniques and we return to a discussion of the experimental results later.

Our motivation for the present work is that we are able to formulate the theoretical equations behind binary fluid mixtures in terms of shell models where the known invariant quantities are conserved. In this way one can investigate the mixture at much higher values of the Reynolds and Prandtl numbers, than is possible by standard numerical simulations. For instance, one can then study the scaling behavior of the mixing time at very high values of the Prandtl number, a regime which might be experimentally accessible. Also, the shell model is known to include intermittency effects, which have not been treated in previous theoretical works on binary fluid mixtures.

With the two fluids labelled A and B, respectively, a scalar field is defined as [6,7]

$$\psi(\mathbf{r}, t) = (\rho_A(\mathbf{r}, t) - \rho_B(\mathbf{r}, t))/\rho_0, \tag{3}$$

where $\rho_A(\mathbf{r}, t)$ and $\rho_B(\mathbf{r}, t)$ are the mass densities of the two fluids and ρ_0 is the mean mass density. In a phase plane determined by the temperature T versus the average of the scalar $\langle\psi\rangle$, there exists a "miscibility-gap" separating the miscible phase from the immiscible. Along this separating curve, the effective diffusivity D vanishes, because it separates a regime where the effective diffusivity is positive (i.e the miscible case) from a regime where it is negative (the immiscible case). Close to the 50–50 % concentrations of the two fluids, one finds in equilibrium

$$\langle\psi(\mathbf{r}, t)\rangle = 0. \tag{4}$$

For this case, as the critical point is approached from the miscible phase, the scalar is supposed to be "active" and influence the velocity equation of the Navier–Stokes equations quite substantially. The corresponding equations of motion were derived almost two decades ago by Siggia et al. [6] and Halperin and Hohenberg [7] and later on elaborated quite a lot by Ruiz and Nelson [8,9]

$$\frac{\partial\psi}{\partial t} + (\mathbf{u}\cdot\nabla)\psi = D\nabla^2\psi, \tag{5}$$

$$\frac{\partial\mathbf{u}}{\partial t} + (\mathbf{u}\cdot\nabla)\mathbf{u} = -\frac{1}{\rho_0}\nabla p' - \alpha\nabla\psi\nabla^2\psi + \nu\nabla^2\mathbf{u} + \mathbf{f}, \tag{6}$$

$$\nabla\cdot\mathbf{u} = 0. \tag{7}$$

Here ν is the kinematic viscosity; $\mathbf{f}$ is the forcing and several terms involving ψ have been incorporated into an effective pressure p' [6,7]. The term with coefficient α represents the "active" part of the scalar. This term acts like a force of the form $\mu_{AB}\nabla\psi$ where $\mu_{AB} = -\alpha\nabla^2\psi$ plays the role of a local chemical potential difference between the A and B component of the mixture [8,9]. The coefficient α has the dimensions of the square of a transport coefficient and has been estimated to be of the order $\alpha \sim \nu^2$ in [8].

The equations of motion (5) and (6) allow two quadratic invariants in the absence of diffusivity, viscosity and forcing, i.e. in the limit $D = \nu = 0, \mathbf{f} = \mathbf{0}$. The first is the squared integral of the concentration fluctuations

$$C_{\text{tot}} = \frac{1}{2}\int \mathrm{d}\mathbf{r}(\psi(\mathbf{r}, t))^2 \tag{8}$$

and the second is the total energy with a term relating to the active influence of the scalar

$$E_{\text{tot}} = \frac{1}{2}\int \mathrm{d}\mathbf{r}(|\mathbf{u}(\mathbf{r}, t)|^2 + \alpha|\nabla\psi(\mathbf{r}, t)|^2). \tag{9}$$

In the case of a passive scalar, i.e. when $\alpha = 0$, one expects the energy spectrum $E(k)$ and the spectrum of the scalar $C(k)$ to have the usual behavior

$$E(k) \sim k^{-5/3-\delta}, \quad C(k) \sim k^{-5/3-\gamma}, \tag{10}$$

where $-5/3$ is the Kolmogorov exponent [10] (and Obukhov–Corrsin [11] exponent for the scalar) and δ and γ are intermittency corrections in the two cases, respectively [12]. Ruiz and Nelson [8,9] also discuss the possibility of internal wave-like excitations, in the case of large values of α, similar to linear wave excitations in MHD, which may change the spectrum to different scaling behavior as predicted by Iroshnikov [13] and Kraichnan [14]. We do not discuss this phenomenon here but reserve it for a forthcoming publication.

An interesting feature of the equations of motion (5) and (6) should be noticed: If the initial velocity field $\mathbf{u}$ vanishes for $t = 0$, then if

$$\nabla\psi \neq 0 \text{ and } \nabla^2\psi \neq 0, \quad \text{and/or} \quad \nabla p' \neq 0 \text{ for } t = 0, \tag{11}$$

it follows from Eq. (6) that a finite velocity field will appear. For small times it is given by

$$\mathbf{u}(\mathbf{x}, t) = -\left(\frac{1}{\rho_0}\nabla p'(\mathbf{x}, 0) + \alpha\nabla\psi(\mathbf{x}, 0)\nabla^2\psi(\mathbf{x}, 0)\right)t + \mathrm{O}(t^2). \tag{12}$$

Here the pressure term should be such as to respect Eq. (7). Eq. (12) means that if initially the liquids are at rest, and experimental initial conditions respecting (11) are established, then one should see that the liquids start to move "spontaneously". This is a very clean effect of a non-vanishing "transport coefficient" α, and it works irrespectively of the magnitude of the diffusion coefficient D. This will be further discussed in Section 7.

The paper is organized as follows. In Section 2 we derive the shell model for turbulent binary fluid mixtures and discuss the corresponding conservation law, the value of the coupling constants, etc. In Section 3 the numerical results obtained from integrating the model are presented. In particular we discuss the appearance of a peak in the spectrum of the scalar. Section 4 contains the theoretical predictions of Ruiz and Nelson for the mixing times and the corresponding results from the shell model. In Section 5 we present the continuum version of the "GOY" model and exact analytic solutions in the inertial range, based on a scaling ansatz. In Section 6 the corresponding continuum equations for the binary mixture model are derived and in Section 7 the numerical results from integrating these equations are presented together with a comparison with the results from the discrete equations. Finally, Section 8 offers concluding remarks.

2. A shell model for binary mixtures

Since the binary mixtures are particularly interesting to investigate in the critical regime where $Pr \to \infty$ and as we are concerned with the case of a strongly turbulent mixture (large values of Re), it is our goal to formulate an approximate scheme for Eqs. (5) and (6) in which this limit is accessible. Shell models in Fourier space fulfill these requirements. They have been introduced by Obukhov [15], Gledzer [16], Desnyansky and Novikov [17]. The key idea is to mimic the Navier–Stokes equations by a dynamical system with N variables $u_1, u_2, \ldots, u_N$, each of which represents the typical magnitude of the velocity field on a certain length scale. The Fourier space is divided in N shells and each shell consists of the set of wave vectors $\mathbf{k}$ such that $k_0 r^n < |\mathbf{k}| < k_0 r^{n+1}$. The variable u_n is the velocity difference over a length $\sim k_n^{-1}$ so that there is only one degree of freedom per shell [12]. Also models with a large number of degrees of freedom have been introduced and analyzed [18,19]. The most studied model is the "GOY" model introduced by Ohkitani and Yamada [20] which was found to be intermittent by Jensen et al. [21] and studied extensively in many other contexts [22–27]. This model uses a complex set of variables and has the

same type of quadratic nonlinearities and the same symmetries as the 3D Navier–Stokes equations. We shall apply the same approach in this paper by expanding the "GOY" model to include the term of the active scalar and at the same time conserve the two different quadratic nonlinearities (8) and (9).

Firstly, we write down the shell model for the scalar equation (5) [8,28]. Using a complex field ψ_n associated to shell n, the equation becomes

$$\left(\frac{\mathrm{d}}{\mathrm{d}t} + Dk_n^2\right)\psi_n = \mathrm{i}[e_n k_n (u_{n-1}^* \psi_{n+1}^* - u_{n+1}^* \psi_{n-1}^*) + g_n k_{n-1}(u_{n-2}^* \psi_{n-1}^* + u_{n-1}^* \psi_{n-2}^*) + h_n k_{n+1}(u_{n+1}^* \psi_{n+2}^* + u_{n+2}^* \psi_{n+1}^*)], \tag{13}$$

where D is the molecular diffusion. The physical time scale of the model is determined by the constant $k_1 = rk_0$, which represents the inverse scale of the largest eddy, and the related velocity $|u_1|$. This time scale is therefore the corresponding eddy-turn-over time $1/(k_1|u_1|)$. In the following, "time unit" thus means this time scale.

The coefficients of the advective terms follow from demanding the conservation of $\sum_n |\psi_n|^2$ when the diffusivity is vanishing $D = 0$. A possible choice is

$$e_n = \frac{1}{r}, \qquad g_n = -\frac{1}{r}, \qquad h_n = \frac{1}{r} \tag{14}$$

with

$$e_1 = e_N = g_1 = g_2 = h_{N-1} = h_N = 0. \tag{15}$$

The shell model equations for (6) will consist of two contributions; the first part is the usual "GOY" shell model [20] (with coefficients a_n, b_n, c_n) and the second part is the shell expression for the "active" term in the velocity equation (6)

$$\left(\frac{\mathrm{d}}{\mathrm{d}t} + \nu k_n^2\right)u_n = \mathrm{i}k_n[a_n u_{n+1}^* u_{n+2}^* + b_n u_{n-1}^* u_{n+1}^* + c_n u_{n-1}^* u_{n-2}^*] + \mathrm{i}\alpha k_n^3[r_n \psi_{n+1}^* \psi_{n+2}^* + s_n \psi_{n-1}^* \psi_{n+1}^* + t_n \psi_{n-1}^* \psi_{n-2}^*] + f\delta_{n,4} \tag{16}$$

with $n = 1, \ldots, N$, $k_n = r^n k_0$ and boundary conditions

$$b_1 = b_N = c_1 = c_2 = a_{N-1} = a_N = s_1 = s_N = t_1 = t_2 = r_{N-1} = r_N = 0. \tag{17}$$

In order to ensure the conservation of the quadratic quantity

$$E_{\mathrm{tot}} = \sum_n (|u_n|^2 + \alpha k_n^2 |\psi_n|^2) \tag{18}$$

in the limit without viscosity, diffusivity and forcing, $\nu = D = f = 0$, one multiplies Eq. (16) by u_n and multiplies Eq. (13) by ψ_n and then balances the terms. The nonlinear terms in u_n lead to the usual constraints of the "GOY" model [12]

$$a_n = 1, \quad b_n = -\frac{\delta}{r}, \quad c_n = -\frac{1-\delta}{r^2}. \tag{19}$$

For the second part of Eq. (16) one balances the terms by the corresponding terms in the scalar equation. With the choice of the parameters (14) we then obtain the following conditions for the coefficients:

$$r_n = r^4 - r^2, \quad s_n = r - r^{-3}, \quad t_n = r^{-4} - r^{-6}. \tag{20}$$

One observes that when the coupling constants for the scalar equation are given (14), then the coefficients of the "active" terms are fixed. As these active terms are proportional to k_n^3, we expect the effects of this term to show up at the end of the spectrum for large values of k_n.

3. Results from the shell model

This section contains some of the numerical results obtained from integrations of the shell model for the binary mixture, derived above. In the simulations we use the standard separation between the shells, $r = 2$, such that $k_n = 2^n k_0$. We apply the "symmetric choice" of the "GOY" parameters, $\delta = 1/2$. In this case it is known that for the "GOY" model alone, the second quadratic invariant assumes the symmetry of a helicity [22], and for that case the model is strongly intermittent and gives results in good agreement with experiments. We study the model with $N = 14$ and 19 shells, $k_0 = 2^{-4}$, and the strength of the forcing term in (16) is $f = 0.005(1+\mathrm{i})$. As argued by Ruiz and Nelson [8,9] the coupling constant of the active term α, has the dimensions of a square of a transport coefficient and is in the order of magnitude

$$\alpha \sim \nu^2. \tag{21}$$

The spectrum of the scalar for the shell variables is defined as

$$C(k_n) = \langle |\psi_n|^2 \rangle / k_n. \tag{22}$$

The brackets stand for averages over initial conditions and time. Similarly, the energy spectrum is defined as

$$E(k_n) = \langle |u_n|^2 \rangle / k_n. \tag{23}$$

Since the scalar equations (5) and (13) are not forced, $C(k_n) \to 0$ in the long time limit. Nevertheless, it is possible to obtain intermediate averages over shorter times. This is in contrast to the case of the velocity spectrum $E(k_n)$ where the mean exists for $t \to \infty$ as the velocity equations (6) and (16) are forced. Firstly, we present results when the value of the viscosity is $\nu = 10^{-4}$, meaning that $Re \sim 10^4$. For this value of the viscosity, a shell model with $N = 14$ shells is employed. In order to observe the differences between a passive and an active scalar, we first consider the case $\alpha = 0$. Fig. 1(a) shows the corresponding spectrum $C(k_n)$ on logarithmic scales in the case $Pr = 1$. The spectrum follows quite closely the Obukhov law [11].

Next the Prandtl number is increased to $Pr = 10^3$. The spectrum, shown in Fig. 1(b), is changed and scales for high value of k_n according to the Batchelor law $C(k_n) \sim k_n^{-1}$, which means that with the increased value of the Prandtl number a viscous-convective regime is observed, as expected [8]. When the scalar becomes active, i.e. $\alpha \neq 0$, by introducing the coupling term (21), the spectrum changes completely and a peak develops at the upper end of the spectrum as indicated on the evolution series, Fig. 1(c). The series is initiated in a state where ψ_n is concentrated at a low k_n value. This corresponds to a large scale disturbance, for instance where the fluids A and B are completely separated. After some time, a peak (or, perhaps more appropriate, a "shoulder") develops at large values of k_n as indicated in the figure (each curve is averaged over 200 time units). After further time the peak disappears and the spectrum ends up in $C(k_n) \sim k_n^{-1}$. The final spectrum in Fig. 1(c) represents again an almost stationary situation and does not change significantly during long time. Let us note in passing that time-averaging give results similar to ensemble-averaging, since the dynamics in the phase space of the u_n- and ψ_n-field is strongly chaotic as determined by positive Lyapunov exponents [12].

This peak was predicted by Ruiz and Nelson [9] and also seen in numerical simulations using Markorvian closure equations. In fact, in those simulations the peak appears much more pronounced than compared to our results. We

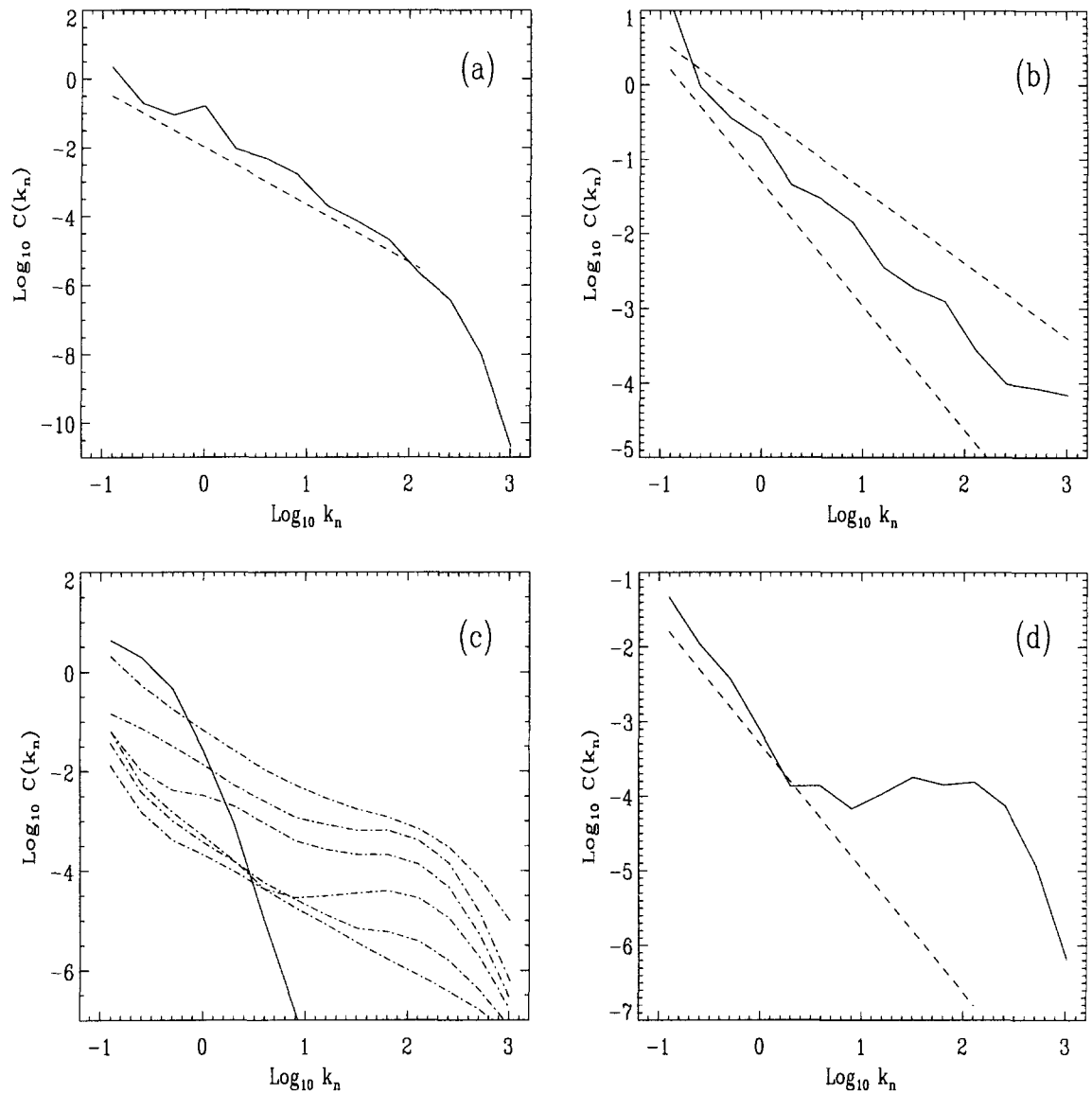

Fig. 1. Results from numerical integrations of the shell model (13) and (16). The parameters are: $N = 14$, $k_0 = 2^{-4}$, $\nu = 10^{-4}$. The spectrum in (a) is averaged over 4000 time units; the other over 200 time units. In the case (a) the spectrum $C(k_n)$ has $D = 10^{-4}$, $Pr = 1$, and $\alpha = 0$. The dashed line in (a) has slope $-5/3$. In the case (b) $D = 10^{-7}$, $Pr = 10^3$, and $\alpha = 0$, and the dashed lines have slopes -1 and $-5/3$, respectively. (c) $C(k_n)$ for $D = 10^{-7}$ and $\alpha = 10^{-8}$. The full curve shows the initial condition. Time progresses from the uppermost spectrum to the lower. The interval between the curves are of the order $\sim$2000 time units. In (d) we show the spectrum at one particular time. The dashed line has slope $-5/3$.

believe the reason is that the strongly intermittent motion could influence the dynamics in a way that the peak becomes less strong. Fig. 1(d) shows one of the spectra in the series indicating the peak more clearly. Note that for low k_n-values, the spectrum is still close to the $-5/3$ law as indicated by the dashed line. The peak indicates that two miscible fluids close to the critical point mix very slowly at the small scales when the fluid is strongly turbulent.

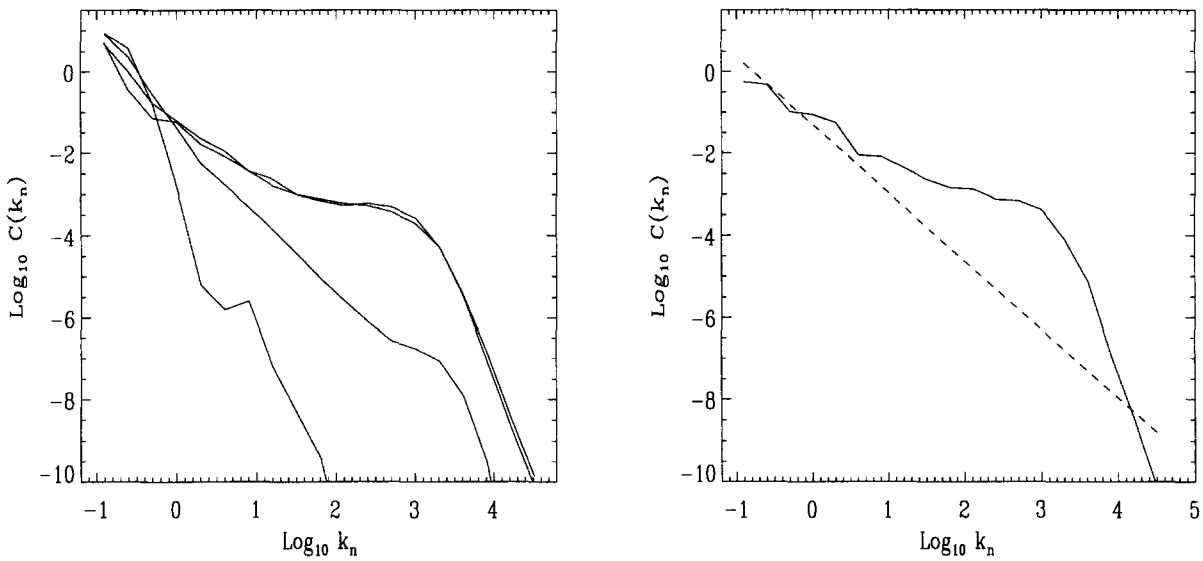

Fig. 2. To the left, spectra $C(k_n)$ obtained from numerical integrations of the shell model, with parameters $N = 19$, $k_0 = 2^{-4}$, $\nu = 10^{-6}$, $D = 10^{-13}$, $\alpha = 10^{-12}$. The different spectra are averaged over four time units and the distance between the spectra are ~ 50 time units. Time progresses from the left to the right. The right-hand figure shows one particular spectrum. The dashed line has slope $-5/3$.

The time for which the peak persists is strongly dependent on the Prandtl and Reynolds numbers. This time is called the mixing time [9].

Fig. 2(a) shows the development of the spectrum $C(k_n)$ for a lower value of the viscosity, $\nu = 10^{-6}$ corresponding to $Re \sim 10^6$. In this case $D = 10^{-13}$ leading to $Pr = 10^7$. Again, starting from an initial condition concentrated on the small k_n-values, one observes the occurrence of the peak at large k_n-values. Fig. 2(b) shows one of the spectra and the dashed line corresponds to $C(k_n) \sim k_n^{-5/3}$. In order to get a more clear picture of the peak, we plot $\langle|\psi_n|\rangle$ versus k_n on logarithmic scales. For a usual Obukhov spectrum one should find $\langle|\psi_n|\rangle \sim k_n^{-1/3}$, whereas for the viscous-convective regime $\langle|\psi_n|\rangle \sim$ const. and the peak will therefore appear more pronounced. Fig. 3 shows the time development of the value of the scalar, where each curve is averaged over 800 time units (the time intervals between the curves are ~8000 time units). One observes that ψ_n is almost constant over the leftmost regime of the spectrum, corresponding to $C(k_n) \sim k_n^{-1}$, whereas the peak is situated at the rightmost part of the spectrum. The peak slowly decreases in intensity (at a rate determined by the mixing time) but for high values of the Prandtl number this decrease occurs extremely slowly: the peak in Fig. 3 diminishes significantly only after about 10^6 time units. Simultaneously, the field as a whole slowly vanishes, $\psi_n \to 0$. This is of course related to the fact that the passive scalar equation (13) is not forced and the input to the motion of ψ_n is only driven by the advective term which includes u_n. Nevertheless, as $Pr \to 0$, $\psi_n \to 0$ slowly, which indeed is reflected in the corresponding value of the mixing time. The presence of a peak appears to be independent of the initial state; one can either, as in Figs. 1 and 2, apply an initial disturbance which is concentrated at the small k_n values, or choose states of ψ_n and u_n which are solutions to the passive scalar equations, i.e. in which $\alpha = 0$. In all cases the result is a peak in ψ_n at large k_n, so an initial perturbation at the large scales is not a necessity in order to observe the enhanced "delay" in the mixing of the two fluids.

In comparison with previous work [8,9], it should be emphasized that in our case the peak is *orders of magnitude smaller* in height. In [9], the peak (after a short time) has a height of order some decades. In our case, as seen from the various figures, the height is only of order half a decade at most, and in many cases it is much less, which could make experimental observations difficult, as indeed appears to be the case [3,5].

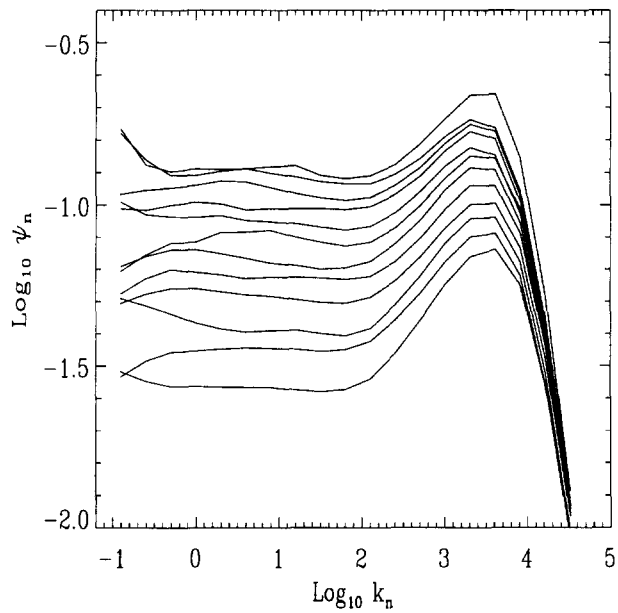

Fig. 3. A plot of $\langle|\psi_n|\rangle$ versus k_n on logarithmic scales. The parameters are $N = 19$, $k_0 = 2^{-4}$, $\nu = 10^{-6}$, $D = 10^{-12}$, and $\alpha = 10^{-12}$. Each curve is averaged over 800 time units and the time intervals between the curves are ~8000 time units. Time progresses from the uppermost curve to the lower.

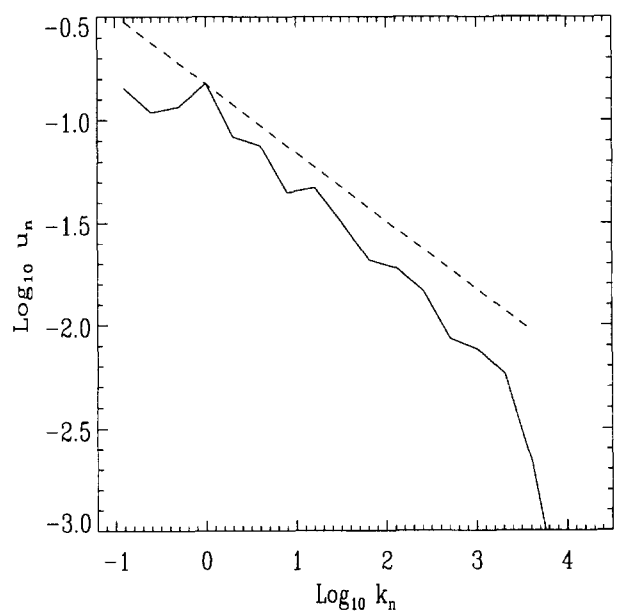

Fig. 4. The velocity spectrum $|u_n|$ versus k_n for the same parameters as in Fig. 3. The spectrum is averaged over ~50 000 time units. The dashed line has a slope $-1/3$.

The corresponding velocity spectrum does not show any sign of a peak, Fig. 4. On the contrary, the cut-off at high wave numbers in the spectrum in fact seems to move to shorter wave numbers (larger scales) as a result of the active coupling. The oscillations in the spectrum is on the other hand much more pronounced than for the usual "GOY" model. This is related to the fact that the motion for the present model is also strongly intermittent and leads to corrections to the Kolmogorov theory. A study of the intermittency effects is reserved to a forthcoming publication.

4. The theoretical predictions by Ruiz and Nelson

Ruiz and Nelson [8,9] have proposed a theory for the dependence of the mixing time on the hydrodynamical parameters. In the case of the passive scalar, $\alpha = 0$, there is not a peak in the spectrum but an inhomogeneity created at the large scale will still persist for a mixing time which is composed of three terms

$$\tau_{\text{pass}} = t_0 + \ln(k'_{\text{d}}/k_{\text{d}}) + \frac{1}{D(k'_{\text{d}})^2}. \tag{24}$$

Here, the first term is the time it takes for a perturbation created at the large scale to reach the dissipative wave number k_{d} (the Kolmogorov length). The second term is the time it takes for a perturbation to go from the dissipative wave number, through the "viscous–convective" regime down to the Batchelor wave number $k'_{\text{d}} = k_{\text{d}} Pr^{1/2}$, and the last term is the time actually needed to dissipate the disturbance at k'_{d}. The second term is found to be of the order $\ln Pr/2Re^{1/2}$. For large values of Re, the mixing time is therefore of the order t_0, unless $\ln Pr \gg Re^{1/2}$ in which case the second term dominates. In the case of an active scalar on the other hand, $\alpha \neq 0$, a peak occurs in the spectrum at a specific wave number k^*, and the last term will therefore dominate when $Pr \gg Re$. The corresponding mixing time is [9]

$$\tau_{\text{active}} \simeq \frac{1}{D(k^*)^2} \simeq t_0 \frac{Pr}{Re}. \tag{25}$$

Also, the wave number of the peak is predicted to be located at $k^* \simeq k_0 Re$, where k_0 is the wave number of an initial perturbation. We observe from this theory, that for large values of the Prandtl number, the mixing time is much longer in the active case than in the passive case.

We have tested the prediction of the theory given by Eq. (25) using the shell model introduced in the previous sections. Fig. 5 shows a plot of the mixing time τ_{active} versus the Prandtl number for two different values of the Reynolds number. In the first case, $Re \sim 10^6$ and Pr in the range from 10^2 to 10^6 and in the second, $Re \sim 10^4$ and Pr in the range 10–10^5. The mixing time is estimated in the following way. At the shell corresponding to the k_n-value on which the maximum of the peak is localized, we monitor the value of $\langle |\psi_n| \rangle$, where the average is over a specific time interval. As this value decreases below a chosen gate ψ_{G}, the corresponding time is associated with the mixing time τ_{active}, at that particular value of the Prandtl number. Then the value of Pr is changed and starting from the same initial conditions, using the same value of the gate, one obtains the new value of τ_{active}, and so on. The mixing time clearly diverges with the Prandtl number as a power law, $\tau_{\text{active}} \sim Pr^{\beta}$. The best fit to the data produces a value $\beta \sim 0.9$ for $Re \sim 10^6$ (as indicated by the dashed line) and $\beta \sim 0.95$ for $Re \sim 10^4$. The prediction (25) of Ruiz and Nelson is valid in the limit $Pr \gg Re$ and this only holds for our data where $Re \sim 10^4$, so the agreement with the theory is reasonable. It is however tempting to conjecture that the presence of intermittency might cause the exponent β to decrease below 1. The shell model presented here in Eqs. (13) and (16) exhibits strongly intermittent motion where the laminar periods are interrupted by bursts of violent motion. The higher the Reynolds number, the more pronounced is the intermittency and since the largest deviations from the prediction (25) is observed at $Re \sim 10^6$, the effects of intermittency could diminish the value of mixing time due to the presence of the long laminar periods.

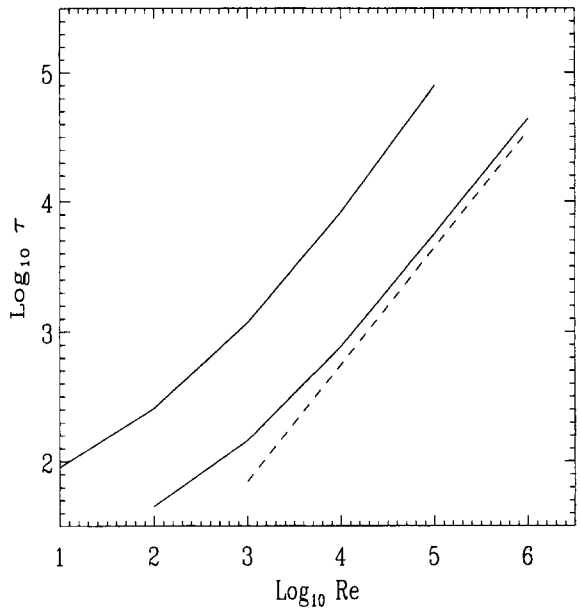

Fig. 5. The mixing time τ_{active} versus the Prandtl number Pr estimated from numerical calculations of shell model with the following parameters: Upper curve: $N = 16$, $k_0 = 2^{-4}$, $\nu = 10^{-4}$, $\alpha = 10^{-8}$ and the gate $\psi_G = 10^{-6}$. Lower curve: $N = 19$, $k_0 = 2^{-4}$, $\nu = 10^{-6}$, $\alpha = 10^{-12}$, and the gate $\psi_G = 10^{-4}$. The slope of the dashed line is 0.9.

Goldburg and coworkers investigated in several experiments the possible existence of the active coupling term in binary mixtures. In [2] the presence of an active term was expected because the mixing time was found experimentally to increase dramatically with the value of the Reynolds number. Nevertheless, the experimental data did not follow the prediction (25). Later experiments showed, however, that the long mixing times were caused by the fact that stirring of the binary mixture cools it down below the critical temperature, into the region where the system is immiscible and phase separation is favored [3]. Subsequent measurements on phase separations and the correlation functions of temporal fluctuations did not show any sign of an anomalous peak in the spectra [4,5]. In [5] it was already argued that intermittency effects might strongly influence the critical fluctuations leading to correlation functions which are stretched exponentials. That intermittency effects are very important close to the critical point is in accordance with the results presented in this paper. Conclusively, one must therefore say that, in spite of several experimental attempts, there is no clear evidence for the active coupling term in (6). We return to this point in Sections 7 and 8.

5. The continuous cascade model for hydrodynamics

The Kolmogorov scaling behavior is a static solution of the energy cascade model. In this section we discuss time-dependent generalizations of the simple $k^{-5/3}$ Kolmogorov behavior of the power spectrum, using a continuous version of the cascade model first discussed by Parisi [26]. Initially these spectra start out as an arbitrary power behavior k^{2p-1}, where p is some constant which can be selected as one wishes (if one includes necessary cutoffs in k-space), but it turns out that after a short time the large k behavior becomes of the Kolmogorov type, with some time dependence. Thus, at a given time the spectra have a "two-slope" structure with a smooth interpolation. The solution is only valid in the inertial range, where diffusion can be ignored.

The simplest hydrodynamical cascade model is given by the equation of motion [20],

$$(\mathrm{d}u_n/\mathrm{d}t + \nu k^2 u_n)^* = -\mathrm{i}k_n \left(u_{n+1}u_{n+2} - \frac{\delta}{r} u_{n-1}u_{n+1} - \frac{1-\delta}{r^2} u_{n-1}u_{n-2} \right) + F_n, \tag{26}$$

where F_n represents an external forcing. From the point of view of energy (i.e. $\sum |u_n|^2$) conservation the parameter δ is arbitrary, but it can be fixed by requiring conservation of (generalized) helicity [22]. In our case we keep the parameter δ arbitrary.

Some years ago Parisi [26] studied Eq. (26) in the limit[2] $r \to 1$, meaning that the distance between the shells goes to zero. Taking $r = 1 + \epsilon$ it is easily seen that one gets

$$\left(\frac{\partial}{\partial t} + \nu k^2 \right) u^* = -\mathrm{i}\epsilon(2-\delta)k \left(u^2 + 3ku\frac{\partial u}{\partial k} \right) + F(k) + \mathrm{O}(\epsilon^2). \tag{27}$$

One might consider this equation to be a "model of a model", and thus very academic. However, as we shall see, this model and, in particular, its generalizations, satisfy the same conservation laws as the corresponding discrete models. Therefore one can equally well consider the continuous version as a model in its own right, with the advantage that it is considerably simpler than the discrete versions.

We can now scale $\epsilon(2-\delta)$ into time t and then let[3] $\epsilon \to 0$. As just mentioned, the resulting model can be considered as being independent of the discrete version, since it satisfies the relevant conservation laws. Instead, one can consider Eq. (27) to be an approximation to the discrete model, to be supplemented by higher order terms in ϵ if needed.

We shall study Eq. (27) in the inertial range, where viscosity can be ignored.[4] Also, we disregard the possible forcing term, so it is then clear that the motion must die out after some time if diffusion is included. Hence we study the equation

$$\frac{\partial u^*}{\partial t} = -\mathrm{i}k \left(u^2 + 3ku\frac{\partial u}{\partial k} \right) + \mathrm{O}(\epsilon). \tag{28}$$

We now choose a special phase and make the ansatz $u = \mathrm{i}k^p f(k^q t)$. Inserting this in Eq. (28) we obtain $q = 1 + p$, i.e.

$$u = \mathrm{i}k^p f(k^{1+p} t). \tag{29}$$

This scaling was first considered by Parisi [26], except for the special case $p = 1$, which was introduced many years ago by Heisenberg [29]. It solves the discrete as well as the continuous model.

A scaling of the type (29) is consistent with the well known invariance of the Navier–Stokes equations (see for instance [30]),

$$l \to \lambda l, \quad u \to \lambda^h u, \quad t \to \lambda^{1-h} t, \quad \nu \to \lambda^{1+h} \nu, \tag{30}$$

in the inertial range, where we can take $\nu = 0$. The reason for this is that the self-similarity (30) can be translated to k-space with $l \to 1/k$, and it then corresponds to the scaling (29) with $p = -h$. The main point is that the scaling variable $k^{1+p}t$ is then an invariant. Also, in the scaling (30) l is usually interpreted as the scale of an eddy, and the typical velocity of this eddy is then $|\mathbf{u}(\mathbf{x}+\mathbf{l}) - \mathbf{u}(\mathbf{x})|$. This compares excellently to the velocity mode u_n

[2] In [8] this limit was considered for a different type of shell model. The resulting equation is linear, in contrast to those considered in this paper.

[3] There exists the possibility of taking the more exotic limit $|\epsilon(2-\delta)| \to$ a finite value, so that $|\delta|$ approaches infinity.

[4] For the special case $p = 1$ we shall include diffusion later in this section.

used in k-space, where u_n is the velocity increment over an eddy of scale $l \sim 1/k_n$. Let us further note that for $p = -h = 1$, diffusion can be included, since (30) then leaves ν invariant.

It should be emphasized that expression (29) has the explicit power k^p in front to accommodate the self-similarity transformation (30) for u. However, the function f depends only on the quantity $k^{1+p}t$, which is *invariant* under the self-similarity transformations (30). In the absence of a solution for f, this function can be completely arbitrary from the point of view of self-similarity, and hence, e.g. the time evolution cannot be predicted at all. This implies that a priori there is *no* agreement with K41 theory (see [30] for a general discussion of K41). Of course, having a solution for f changes the situation.

Eq. (29) thus means that the velocity mode is initially assumed to be of the form k^p. Physically, one can imagine that this initial condition is produced by some external force. In this sense the selection of initial conditions is equivalent to initial forcing. Also, p governs the initial correlation function $\langle u_i(\mathbf{x})u_k(\mathbf{y})\rangle$. The cases $p = 3/2$ or 1 correspond to Gaussian disorder in three and two dimensions, respectively, i.e. $\langle u_i(\mathbf{x})u_k(\mathbf{y})\rangle \propto \delta_{ik}\delta^3(\mathbf{x}-\mathbf{y})$ or $\delta_{ik}\delta^2(\mathbf{x}-\mathbf{y})$, respectively.[5] This is because the k-space energy spectrum is given by

$$E(k,t) = |u(k,t)|^2/k = \text{const}\, k^{D-1} \int \mathrm{d}^D x \exp(\mathrm{i}\mathbf{k}\mathbf{x})\langle \mathbf{u}(\mathbf{x},t)\mathbf{u}(0,t)\rangle, \tag{31}$$

in D dimensions.

In order to have an convergent energy

$$E = \int \mathrm{d}k|u|^2/k, \tag{32}$$

we obviously need an ultraviolet cutoff for $p \geq 1/2$. Similarly, for $p \leq 0$ an infrared cutoff is needed.

At this stage we need a discussion of the boundary conditions associated with (27) and (28). From (27) we get energy conservation in the absence of forcing and viscosity provided

$$k|u(k,t)|^3 \to 0 \quad \text{for } k \to 0 \text{ and } \infty. \tag{33}$$

If this condition[6] is not satisfied for $k \to \infty$ there is "diffusion at infinity" [26].

Inserting (29) in Eq. (28), we obtain the following equation for f:

$$\frac{\mathrm{d}f(x)}{\mathrm{d}x} = -\frac{(1+3p)f(x)^2}{1+3(1+p)xf(x)}, \quad x = k^{1+p}t. \tag{34}$$

This equation can be simplified by the substitution

$$f(x) = g(x)/x, \tag{35}$$

and we get

$$\frac{\mathrm{d}g(x)}{\mathrm{d}\ln x} = \frac{g(x)+2g(x)^2}{1+3(1+p)g(x)}. \tag{36}$$

The solution is given by

$$g(x)(1+2g(x))^{(1+3p)/2} = x/x_0. \tag{37}$$

[5] Here we leave out a discussion of the consequences of $\mathrm{div}\,\mathbf{u} = 0$, which requires a projection operator in the definition of Gaussian randomness. This is of no relevance in the following.

[6] In the discrete version (26) there is, strictly speaking, a similar boundary condition if n goes to infinity. This is because when one checks energy conservation, sums of the type $\sum^{\infty} k_n uuu$ (the u's have different indices) are encountered. Although there is a complete cancellation of these terms, the sums only exist in a strict mathematical sense if all terms of the type $k_n uuu$ vanish for $n \to \infty$.

Here x_0 is an arbitrary constant which gives the strength of the initial velocity mode,

$$u(k,0) = \mathrm{i}k^p/x_0. \tag{38}$$

When $x \to \infty$ we find from (37) that

$$g(x) \to 2^{-(1+3p)/3(1+p)}\,(x/x_0)^{2/3(1+p)}. \tag{39}$$

Inserting this in (29) and (37) we get

$$|u(k,t)| \to 2 - (1+3p)/3(1+p)x_0 - 2/3(1+p)t - (1+3p)/3(1+p)k - 1/3. \tag{40}$$

Thus we see that irrespective of the initial spectrum (38) the velocity approaches the Kolmogorov spectrum with a time-dependent amplitude for large values of k and/or time. Note that this decay law does not agree with the classical theory put forward by Karman and Howarth [31] and Kolmogorov [10] which is of course due to the non-triviality of the function f in (29) (see the general discussion on classical results on decay laws by Frisch [30]).

There are a few special cases where Eq. (37) can be solved explicitly. The simplest is the case where $p = -1/3$, where we get $g(x) = x/x_0$, leading to the time-independent Kolmogorov spectrum,

$$|u(k,t)| = k^{-1/3}/x_0, \quad \text{for } p = -1/3. \tag{41}$$

This result is trivial, since it is easy to see that the original equation (28) has (41) as a static solution.

A non-trivial result can be obtained by considering the case $p = 1/3$, where Eq. (37) becomes second order in g. Using (29) and (35) we then obtain

$$|u(k,t)| = \frac{1}{4kt}\left(-1 + \sqrt{1 + 8k^{4/3}t/x_0}\right). \tag{42}$$

For small but non-vanishing t, the slope in the corresponding power spectrum changes from $-1/3$ to $-5/3$. For $k \to \infty$ the boundary condition (33) is not satisfied. This is simply a consequence of the fact that the Kolmogorov spectrum does not satisfy this condition. As mentioned before, we only expect the solution (42) to be relevant for the inertial range, where diffusion is negligible. For completeness we mention that the energy integrated to $k = \infty$ is given by

$$E = \sqrt{2}/(x_0^2\sqrt{t}). \tag{43}$$

The energy content approaches zero as time goes on simply because the class of solutions (29) correspond to an inverse cascade moving towards smaller values of k, ultimately reaching the value 0 except in the point $k = 0$, where it is given by $1/x_0^2$. In "**x**-space" this means that small scale structures in time become structures of infinite extension, with no local energy. This shows up if we consider the "integral scale" l_0 used in turbulence theory as a measure of possible large scale structures,

$$l_0 = \int \frac{\mathrm{d}k}{k} E(k) \left(\int \mathrm{d}k\, E(k)\right)^{-1} \quad \text{with } E(k) = |u|^2/k. \tag{44}$$

This quantity behaves like $t^{3/4}$, and in the general case it goes as $t^{1/(1+p)}$. Hence, for large times the structures become very extended.

Another case which can be solved is $p = 1$, since Eq. (37) then becomes a cubic equation for g. We find

$$|u(k,t)| = R(s)/kt, \tag{45}$$

where

$$R(s) = \frac{1}{6}\left(\left(1+s\left(1+\sqrt{1+\frac{2}{s}}\right)\right)^{1/3} + \left(1+s\left(1+\sqrt{1+\frac{2}{s}}\right)\right)^{-1/3} - 2\right), \tag{46}$$

and

$$s = 27k^2 t/x_0. \tag{47}$$

The energy spectrum initially has the slope $+1$. For small k the slope remains $+1$, but at larger values of k the slope turns into $-5/3$, in accordance with the universality of the Kolmogorov spectrum at large k's. Again there is an inverse cascade moving the energy towards smaller k's as time passes.

The $p = 1$ case is interesting from the point of view of studying the effect of diffusion. The main feature is that in general the ansatz (29) is not consistent with the viscosity term on the left-hand side of Eq. (27). However, when $p = 1$, the powers of k nicely divide out on both sides of Eq. (27), leaving them as functions of the scaling variable x only. Instead of Eq. (34) we obtain

$$\frac{\mathrm{d}f(x)}{\mathrm{d}x} = -\frac{4f(x)^2 + \nu f(x)}{1 + 6xf(x)}. \tag{48}$$

The substitution (35) cannot be used to solve this equation because of the dissipative term. However, Eq. (48) can of course easily be solved numerically, and the result compared to the analytic solution (46). To see the effects expected, let us compute the diffusion cutoff defined by $f^2 \sim \nu f$ (see Eq. (48)), using Eqs. (29), (35) and (39) applied to the case $p = 1$,

$$x_{\mathrm{D}} \sim x_0^{-1/2}\nu^{-3/2} \quad \text{or} \quad k_{\mathrm{D}} \sim \nu^{-3/4}x_0^{-1/4}t^{-1/2}, \tag{49}$$

which is what one expects as far as the dependence on ν is concerned. However, the time dependence should be noticed. The latter reflects the fact that we have an inverse cascade. The cutoff (49) is in qualitative agreement with what one obtains by comparing the analytic solution (46) with the numerical solution of (48). In Fig. 6 we give an example of a solution, where we plot the energy. It is clearly seen that there is a change from the initial slope $+1$ to $-5/3$.

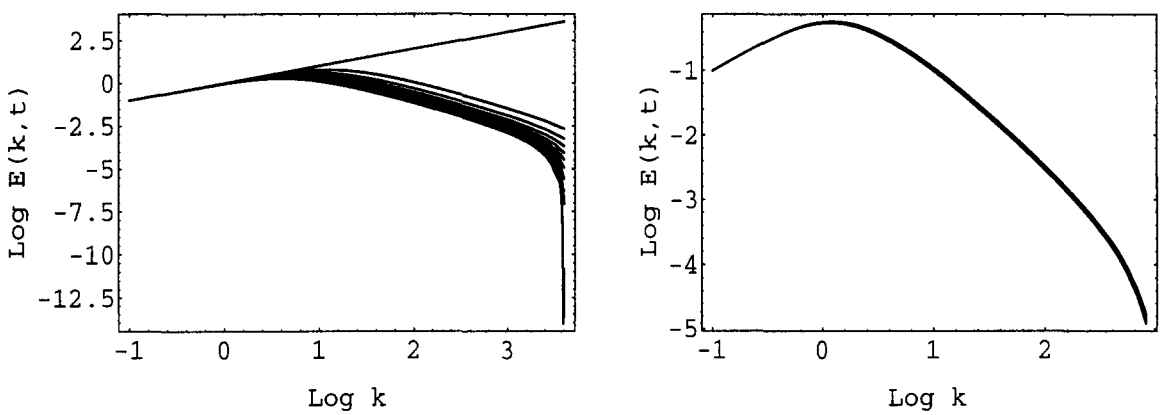

Fig. 6. A double logarithmic (base 10) plot of the energy spectrum $E(k,t)$ as a function of k in the continuous model. In the left-hand figure we show 10 small values of time, from $t = 0$ (where the E goes like k) to $t = 10^{-2}$. In the right-hand figure we show E for 10 values of time between $t = 1$ and $t = 1.1$. In both cases time moves from the right to the left. The viscosity is $\nu = 10^{-2}$, $x_0 = 1$, and from (49) $\log_{10} k_D$ is of order 2.5 (left) and 2 (right), in reasonable agreement with the figures.

For a general p the result (49) can be extended to

$$k_D \sim \nu^{-3/4} x_0^{-1/2(1+p)} t^{-(1+3p)/4(1+p)}. \tag{50}$$

The behavior of k_D as a function of ν is thus universal, i.e. independent of p, whereas the time dependence of k_D is clearly non-universal.

Results (49) and (50) are to some extent consistent with Kolmogorov's scaling arguments as far as the ν-dependence *and* as far as the time dependence are concerned. The energy should go as $E(k) \sim \epsilon^{2/3} k^{-5/3}$, where ϵ is the kinetic energy per unit mass (anyhow put equal to one) and time, with $\epsilon = \mathrm{d}E/\mathrm{d}t \sim ku^3$ for large k. Now from (40) $ku^3 \sim t^{-(1+3p)/(1+p)}$ for large k. From Kolmogorov's arguments one expects the dissipation scale $k_D \sim \nu^{-3/4}\epsilon^{1/4}$, i.e. $k_D \sim \nu^{-3/4} t^{-(1+3p)/4(1+p)}$. This is exactly result (50), also as far as the time dependence is concerned. Of course, the fact that ϵ is not a constant in our case, does not conform to Kolmogorov's argument.

In the case $p = 1$ it is possible to obtain an implicit equation for $g(x)$ even when diffusion is included. For $\nu \neq 0$, proceeding like in Eqs. (34)–(37) and (46) we get that Eq. (37) is replaced by

$$g(k^2t)(1 + 2g(k^2t))^2 = \frac{k^2 t}{x_0} \exp\left(-\nu \int_0^{k^2 t} \mathrm{d}x \frac{1}{1 + 2g(x)} \right). \tag{51}$$

Therefore Eq. (45) is changed to

$$|u(k,t)| = R(d)/kt, \tag{52}$$

where $R(d)$ is given by (46), and where

$$d = \frac{27k^2 t}{x_0} \exp\left(-\nu \int_0^{k^2 t} \mathrm{d}x \frac{1}{1 + 2g(x)} \right). \tag{53}$$

This equation can be used iteratively, starting from the behavior for $\nu = 0$. To the lowest non-trivial order in ν Eq. (52) becomes

$$|u(k,t)| = R(27k^2 t \exp(-\nu k^2 t)/x_0)/kt \tag{54}$$

for $k^2 t$ small. It is interesting that (54) is a self-consistent solution of Eq. (51) for $k^2 t$ small and large. Thus the decay of the velocity at large k is exponential. For $k^2 t$ neither small or large, the expression given by (46) and (53) indicates that an exact inclusion of diffusion is rather complex, even in this simple model.

It is very interesting that the scaling behavior for the case $p = 1$, i.e. $u(k,t) = kf(k^2 t)$ was first considered by Heisenberg in his model, where in the range from 0 to k, the action of all smaller eddies are assumed to be represented by an effective viscosity [29]. Although it is not obvious that the cascade model satisfies this assumption, the Heisenberg scaling appears as a solution. Physically the $k^2 t$-scaling can be understood [29] by assuming that the spectrum is determined by one length only, namely the length $\sim 1/k_0$ of the largest eddies. Let the velocity of these eddies be v_0. On dimensional grounds it then follows that [29]

$$\frac{\mathrm{d}}{\mathrm{d}t}(1/k_0) \sim v_0, \quad \text{and} \quad \frac{\mathrm{d}}{\mathrm{d}t}(1/v_0) \sim k_0, \tag{55}$$

from which one gets $k_0 \sim v_0 \sim 1/\sqrt{t}$. This is exactly the scaling in the $p = 1$ case. However, the continuous model has an exponential decay for large k, in contrast to Heisenberg's model, which has a power behavior, presumed to be unrealistic [12].

The solutions discussed above refer to the case when the phase is fixed. One can try to find solutions where the phase plays a dynamical role by making the scaling ansatz $u = \mathrm{i}k^p f(k^{1+p})$ with f a complex function, in which case Eq. (34) is replaced by

$$\frac{\mathrm{d}f^*(x)}{\mathrm{d}x} = -3(1+p)xf(x)\frac{\mathrm{d}f(x)}{\mathrm{d}x} - (1+3p)f(x)^2. \tag{56}$$

For the case $p = 1/3$, introducing again the substitution (35) with $g(x)$ complex, this leads to the result

$$g^*(x) + 2g(x)^2 = x/x_0, \quad x = k^{4/3}t. \tag{57}$$

This equation has the previously discussed real solution corresponding to (42), as well as a new complex solution with

$$\mathrm{Re}\, g(x) = 1/4, \qquad \mathrm{Im}\, g(x) = \sqrt{(3 - 8x/x_0)}/4. \tag{58}$$

This solution is obviously only valid for $x \leq 3/8x_0$. Since x can take any value from 0 to ∞ the complex solution should be rejected.

To summarize the results obtained so far, one can say that the continuous model gives interesting, non-trivial results. This model is most interesting for the case where $p = 1$, since then diffusion can be included. The initial condition $|u(k, 0)| \propto k$ then corresponds to an initial Gaussian disorder in two dimensions. Therefore we believe that this model may be of most relevance in two dimensions. This is consistent with the fact that the model has an *inverse* cascade.

There exists a generalization to a model with helicity, namely the continuous version of a model introduced by Biferale and Kerr [27], leading to [12]

$$\left(\frac{\partial}{\partial t} + \nu k^2\right)(u^+)^* = -\mathrm{i}k\left(4ku^-\frac{\partial u^+}{\partial k} + 2ku^+\frac{\partial u^-}{\partial k} + (2+\alpha)u^+u^- - \alpha(u^-)^2\right). \tag{59}$$

There is a similar equation with $+ \leftrightarrow -$. The energy and the generalized helicity are conserved,

$$E = \int \frac{\mathrm{d}k}{k}(|u^+|^2 + |u^-|^2), \qquad H = \int \frac{\mathrm{d}k}{k}k^\alpha(|u^+|^2 - |u^-|^2). \tag{60}$$

Making the scaling ansatz

$$u^+ = \mathrm{i}k^p f(k^{1+p}t) \quad \text{and} \quad u^- = \mathrm{i}k^p\, h(k^{1+p}t), \tag{61}$$

one obtains from (59) by ignoring viscosity

$$\frac{\mathrm{d}f(x)}{\mathrm{d}x} = -\frac{2(1+p)xf\,\mathrm{d}h/\mathrm{d}x + (6p+2+\alpha)fh - \alpha h^2}{1+4(1+p)xh}. \tag{62}$$

There is a similar equation with f and g interchanged. These equations have a potentially much richer structure than Eq. (34). We also mention that the discrete and continuous GOY equations have been generalized to magnetohydrodynamics, using a helicity decomposition [32].

6. The continuous shell model for turbulent mixtures

In Section 2 we discussed the shell model for binary mixtures. Proceeding exactly as in Section 5, we can now derive the continuous version of the relevant equations. Here we shall just give the results. For convenience we define $\phi = k\psi$, and after a rescaling of time the equations become

$$\frac{\partial \phi^*}{\partial t} + Dk^2\phi^* = \mathrm{i}k\left(-v\phi + \phi k\frac{\partial v}{\partial k} + 2vk\frac{\partial \phi}{\partial k}\right) \tag{63}$$

and

$$\frac{\partial v^*}{\partial t} + \nu k^2 v^* = \mathrm{i}k\left(2\alpha\phi^2 + c\left(v^2 + 3vk\frac{\partial v}{\partial k}\right)\right). \tag{64}$$

Here v is the velocity mode and c is an arbitrary constant. These equations conserve

$$\sum |\psi_n|^2 \to \int \frac{\mathrm{d}k}{k}|\psi|^2 \quad \text{and} \quad \sum(|v_n|^2 + \alpha|\phi_n|^2) \to \int \frac{\mathrm{d}k}{k}(|v|^2 + \alpha|\phi|^2), \tag{65}$$

provided we have the boundary conditions

$$v|\phi|^2/k \to 0, \quad k|v|^3 \to 0, \quad k|\phi|^2 v \to 0, \tag{66}$$

for $k \to \infty$ and 0. Again there may be "diffusion at infinity", as discussed in Section 5.

We can now look for scaling solutions of Eqs. (63) and (64) in the inertial range. It turns out that they should have the form (analogously to MHD)

$$\phi(k,t) = \mathrm{i}k^a\bar{\phi}(k^{1+a}t) \quad \text{and} \quad v(k,t) = -\mathrm{i}k^a\bar{v}(k^{1+a}t). \tag{67}$$

These results have been found by requiring that powers of k on the two sides of Eqs. (63) and (64) should cancel out. This fixes the powers in v and ϕ to be identical. It is interesting that these results are again consistent with the exact self-similarity of the Navier–Stokes equation (30), supplemented by $\psi \to \lambda^{-a}\psi$, as can be seen from Eq. (6). From Eqs. (63) and (64) we then get

$$-\bar{\phi}'(x)^* = (3a-1)\bar{v}(x)\bar{\phi}(x) + (1+a)x\bar{\phi}(x)\bar{v}'(x) + 2(1+a)x\bar{v}(x)\bar{\phi}'(x) \tag{68}$$

and

$$\bar{v}'(x)^* = -2\alpha\bar{\phi}(x)^2 - c((1+3a)\bar{v}(x)^2 + 3(1+a)x\bar{v}(x)\bar{v}'(x)). \tag{69}$$

Here the scaling variable x is given by $k^{1+p}t$.

In general the scaling ansatz (67) is inconsistent with diffusion, and hence Eqs. (68) and (69) can only be used in the inertial range. However, as already seen in Section 5, the case $a = 1$ is an exception. In this case all powers of k neatly cancel out even in the presence of diffusion. If we assume that the functions $\bar{\phi}$ and $\bar{v}$ are real, the equations become

$$-\bar{\phi}'(x)/\bar{\phi}(x) = (2\bar{v}(x) + 2x\bar{v}'(x) + D)/(1 + 4x\bar{v}(x)) \tag{70}$$

and

$$\bar{v}'(x) = -(2\alpha\bar{\phi}(x)^2 + 4c\bar{v}(x)^2 + \nu\bar{v}(x))/(1 + 6cx\bar{v}(x)), \tag{71}$$

where the scaling variable is now $x = k^2t$.

Eqs. (70) and (71) can be reformulated in a way which is similar to what was done in Section 5. From (70) we get

$$\bar{\phi}(k^2t) = \frac{\bar{\phi}(0)}{\sqrt{1 + 4k^2t\bar{v}(k^2t)}}\exp\left(-D\int_0^{k^2t}\mathrm{d}x/(1 + 4x\bar{v}(x))\right). \tag{72}$$

Similarly Eq. (71) can be integrated to give the implicit equation

$$\bar{v}(k^2t)(1+2ck^2t\bar{v}(k^2t))^2 = \bar{v}(0)\exp\left(-\nu\int_0^{k^2t} \mathrm{d}x \frac{1}{1+2cx\bar{v}(x)}\left(1+\frac{2\alpha}{\nu}\frac{\bar{\phi}(x)^2}{\bar{v}(x)}\right)\right), \tag{73}$$

provided $\bar{v}(0)$ does not vanish. This result is similar to Eq. (51), and a comparison shows that the last factor on the right above (containing $\bar{\phi}^2/\bar{v}$) is very similar to diffusion. Thus in this particular model, the effect of $\bar{\phi}$ on the velocity field is essentially to provide some additional diffusion. Comparing with Section 5, we therefore expect that the Kolmogorov regime for the velocity mode $k\bar{v}$ becomes smaller, since the effective diffusion becomes stronger.

In the inertial range Eqs. (72) and (73) can be explicitly solved analogously to what we did in Section 5. Eq. (73) has the solution

$$\bar{v}(k^2t) = R(27c\bar{v}(0)k^2t)/ck^2t, \tag{74}$$

where R is given by Eq. (46). Eq. (72) then gives

$$\bar{\phi}(k^2t) = \bar{\phi}(0)/\sqrt{1+4R(27c\bar{v}(0)k^2t)/c}. \tag{75}$$

Like in Section 5 it is easy to see that for large k^2t Eqs. (74) and (75) imply the Kolmogorov and Obukhov–Corrsin exponents for the velocity and for the field $\bar{\phi} = \psi$, respectively.

The advantage of the basic equations (70) and (71) is that they are just two ordinary coupled differential equations. Therefore, they are much simpler than the usual large number of coupled cascade equations. However, it should be remembered that the set-up is very special. We need to assume initial ($t = 0$) spectra which are linear in k. Thus, it is not possible to start, e.g. with an initial Gaussian spectrum. However, the results in the discrete cascade model reported in Section 3 indicate that the final results are independent of the initial state. However, in any case one may wonder whether the simplicity has not been achieved at the cost of loosing the physics of the problem. This will be discussed in the next section.

7. Results in the continuous model

In this section we shall compare the continuous cascade model with the discrete one by obtaining qualitative and quantitative results. From the scaling which we introduced for v and ϕ, it is clear that the continuous model will produce an inverse cascade, whereby energy is transferred from large to small k-values. Such a phenomenon is known in magnetohydrodynamics (MHD) for the magnetic energy [33] and in an MHD discrete cascade model [25], where it is presumably due to an inverse cascade in the three-dimensional magnetic helicity (for another shell-model on this point, see [34]). The continuous cascade model for MHD [32] gives results very similar to the discrete model. In this connection, it is of interest that the basic equations used for turbulent mixtures are rather analogous to the MHD-equations.

We begin by a qualitative discussion of the results expected, based on Eqs. (72) and (73). If diffusion is ignored (and $\alpha = 0$) these equations are explicitly solvable. Eq. (74) implies that $\bar{v}$ is given exactly like the velocity u in Section 5, so

$$x\bar{v}(x) \propto x^{1/3} \tag{76}$$

for large values of $x = k^2t$ in a range, where diffusion can still be ignored. From Eq. (75) we then see that the quantity $C(k) = \psi^2/k = \bar{\phi}^2/k$ behaves like $k^{-5/3}$ with the Obukhov–Corrsin exponent (with some time dependence). If

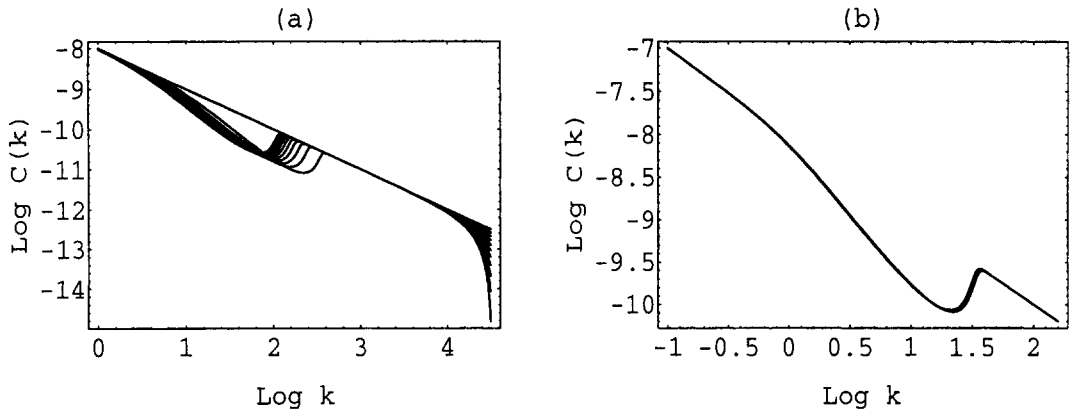

Fig. 7. A double logarithmic (base 10) plot of the spectrum $C(k)$ as a function of k in the continuous model for (a) 10 small values of time, from $t = 0$ (where the C goes like $1/k$) to $t = 10^{-2}$, and (b) for 100 times larger. Time moves from the right to the left.

the Prandtl number $Pr = \nu/D$ is large, diffusion in the first place acts on the velocity. Thus, $x\bar{v}$ starts to decrease, and from (75) it follows that $\bar{\phi}$ approaches its initial value, i.e. $C(k)$ goes like $1/k$ (with some time dependence), which is the Batchelor behavior. Therefore, without doing any numerical calculations, we see from Eqs. (73) and (75) that $C(k)$ must change slope from $-5/3$ to -1. When k becomes so large that the diffusion governed by D is operative, of course $C(k)$ decays exponentially, according to Eq. (72). If, on the other hand, Pr is of order 1 or less, it follows by the same reasoning as given above (based on Eqs. (72) and (73)) that only the $-5/3$ slope materializes itself, before the exponential decays set in. This is in agreement with the results obtained in the discrete model, as discussed in Section 3.

We have made some numerical calculations, using the values

$$\nu = 10^{-1}, \quad D = 10^{-7}, \quad \alpha = \nu^2, \quad Pr = 10^6. \tag{77}$$

The initial values are given by $\bar{v}(0) = 1$ and $\bar{\phi}(0) = 0.0001$. We also took the constant c in Eq. (71) to be 1/2. The results are presented for the spectrum $C(k) = \bar{\phi}^2/k = \psi^2/k$ and the velocity mode $k\bar{v}$. In Fig. 7 we show $C(k)$ for relatively low and for relatively large times. The initial behavior is linear in k (from our initial condition that $\bar{\phi}(0)$ is a constant). From Fig. 7 we see this behavior for $t = 0$. When t increases, the slope changes to $-5/3$ in a range of k-values from approximately 10 to slightly less than 10^2. From Fig. 8 for the velocity mode, we see that at a k-value around 100, the velocity decreases rapidly. Therefore, as one can see from Eq. (72) and as one can also see from Fig. 7(a), after the initial decrease with slope $-5/3$, the spectrum $C(k)$ increases until it regains the Batchelor slope -1. Ultimately, for k slightly above 10^4 one sees that $C(k)$ starts to decrease exponentially. This repeats itself at later times, as is also seen from Fig. 7, but when time increases, the "velocity of change" $k/t \propto 1/\sqrt{t}$ decreases, so the curves for the 10 different times in Fig. 7 are much closer at later times. In the region where C increases (between slope $-5/3$ and slope -1), there are very short range correlations in **x**-space. This could be a rudimentary version of an intermittency fluctuation.

We have also investigated the question of equipartition. For small k the kinetic energy dominates. Around the value of k where the peak appears, there is equipartition in essentially only one point. The energy $E_\psi = \alpha k \psi^2$ then dominates for larger values, where the kinetic energy becomes very small compared to E_ψ. It should also be noticed that the peak is time dependent, and moves towards smaller values of k with a "velocity" $k/t = 1/\sqrt{t}$.

Finally, we have studied the influence of the parameter α. It seems that the continuous model differs from the discrete one with respect to this point. For the various values of Pr and ν we have studied, we find that the influence

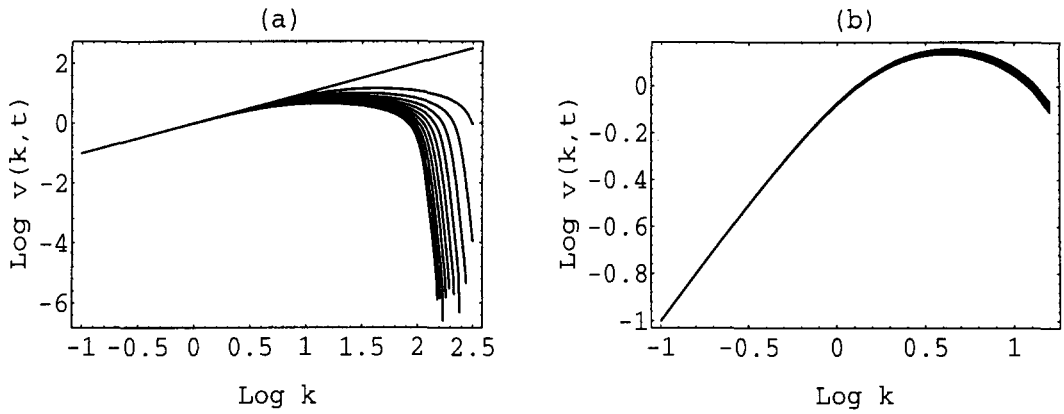

Fig. 8. Double logarithmic plot (base 10) for the velocity mode $v(k,t) = k\bar{v}$ as function of k for (a) 10 time values between 0 (where $v(k,0) = k$) and 10^{-2}, and (b) for 100 times larger times.

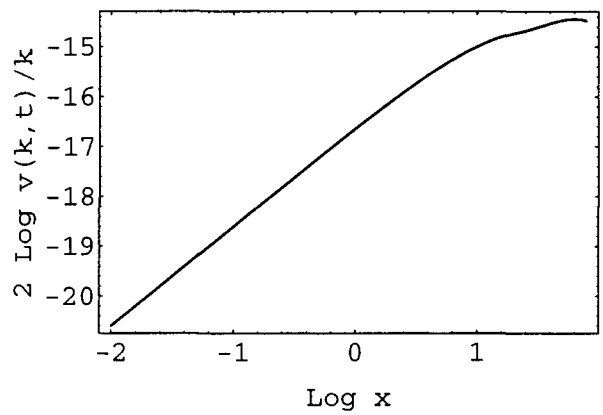

Fig. 9. A log–log plot (base 10) of the scaling function $\bar{v}^2 = (v(k,t)/k)^2$ as a function of the scaling variable $x = k^2 t$ for the initial conditions $\bar{v}(0) = 0$ and $\bar{\phi}(0) = \psi(0) = 0.0005$.

of α is only rather marginal, and we do not find any really spectacular effect of α. It would therefore be interesting to study the case where the initial velocity is zero (or very small). In this case there is no effect (or only a slight effect) if we have a passive scalar, so with α non-vanishing one will see an effect (almost) entirely due to α. This problem can be analyzed from Eqs. (72) and (73) by replacing $\bar{v}(0)$ by $\bar{v}(\epsilon)$ and performing the limit $\epsilon \to 0$ in such a way that $\bar{v}$ approaches zero. We can also study this by analyzing Eq. (71) near $x = 0$, using the boundary condition $\bar{v}(0) = 0$. We get from (71) (compare with Eq. (12))

$$\bar{v}(x) \approx -2\alpha\bar{\phi}(0)^2\, x + \mathrm{O}(x^2). \tag{78}$$

Thus the velocity scaling function must be negative and linear for small values of the scaling variable $x = k^2 t$.

We have also studied this problem numerically. In Fig. 9 we show the resulting scaling function $\bar{v}^2 = v(k,t)^2/k^2$ as a function of the scaling variable. The values of ν and Pr are as used before, but initially we assume $\bar{v}(0) = 0$, and $\bar{\phi}(0) = \psi(0) = 0.0005$. Although the velocity-scaling function is very small, there is clearly an effect. However, the resulting back-reaction on $\bar{\phi}$ is small in most cases. This can be seen from Eq. (72), since the velocity field in the denominator on the right-hand side is small. However, there may exist initial conditions where this is not true,

and where $x\bar{v}(x)$ may approach -1, causing ψ to diverge. In such a case stabilizing terms of higher orders in ψ must be included in the basic equations (5) and (6). Disregarding this possibility, the density function ψ is rather insensitive to velocity fluctuations, when the kinematic viscosity ν is much larger than the viscosity D of ψ. This effect is somewhat similar to what has recently been seen in MHD [32,35] for large "Prandtl" numbers (i.e. for the kinematic viscosity much larger than the Ohmic diffusion).

From an experimental point of view it would be interesting to study the case where the initial velocity vanishes or is small, and where some initial distribution (e.g. random) is established with a non-constant gradient of ψ. The fluids should then be set "spontaneously" in motion. The gradient field is analogous to the magnetic field in MHD. Therefore, such an experimental set-up would be somewhat analogous to the study of primordial magnetic fields in the early universe (see [25,32]), where the magnetic field can induce a velocity field. It would clearly be of interest to investigate this analogy in an earthbound laboratory.

To conclude this section, we do not find the large peak predicted in [9] for increasing Prandtl numbers. There is a small time dependent peak of magnitude less than a half decade, as can be seen, e.g. from Fig. 7. This is to be contrasted with a peak of several decades in [9]. Whether this is a shortcoming of the continuous model is, of course, an experimental question. However, our results are not so different from those of the discrete GOY model, discussed in Section 3, where the peak is of the same order of magnitude as found here. However, the nature of the peak is different in the two cases, since the α dependence differ, as mentioned above.

8. Conclusions

The main result of the present paper is that intermittency effects are likely to play an important role in turbulent binary fluids. The influence of intermittency is not small; compared to previous studies of non-intermittent binary fluids [8,9] the peak in the concentration spectrum is much less pronounced and less persistent because the fluctuations tend to "surround" and diminish the peak. It is therefore not easy to see the effect of the active coupling term (6) from the spectra, in accordance with experiments [3–5]. The transport coefficient α in (6) presumably has its most dramatic effect in the case where the initial velocity vanishes. Here the existence of a non-vanishing α implies the "spontaneous" generation of a velocity field, provided there is an initial variation in the gradient of ψ. The observation of such an effect would have an analogy in MHD, where an initial ("primordial") magnetic field induces a velocity field, which may be of relevance in the early universe. On the other hand, if such an effect is not observed in binary mixtures, this would indicate that the active coupling term (6) is probably not present. If so, binary mixtures would not be analogous to MHD.

Also, we see that the continuous model gives results which are rather similar to the discrete model. In the continuous case there also exists a time-dependent peak.

Acknowledgements

We thank David R. Nelson and Walter Goldburg for stimulating discussions. We also thank George Savvidy for reminding us of Heisenberg's paper [29], and Yuri Makeenko for much help in inserting the figures.

References

[1] H.L. Swinney and D.L. Henry, Phys. Rev. A 8 (1973) 2586.
[2] J.V. Maher, N. Easwar, W.I. Goldburg and M. Joshua, Phys. Rev. Lett. 49 1850 (1982); N. Easwar, J.V. Maher, D.J. Pine and W.I. Goldburg, Phys. Rev. Lett. 51 1272 (1983), N. Easwar, M. Joshua, J.V. Maher and W.I. Goldburg, Physica A 118 (1983) 268.

[3] C.K. Chan, J.V. Maher and W.I. Goldburg, Phys. Rev. A 32 (1985) 3117.
[4] C.K. Chan and W.I. Goldburg, Phys. Rev. Lett. 58 (1987) 674.
[5] P. Tong, W.I. Goldburg, J. Stavans and A. Onuki, Phys. Rev. Lett. 62 (1989) 2268; K.Y. Min, J. Stavans, R. Piazza and W.I. Goldburg, Phys. Rev. Lett. 63 (1989) 1070.
[6] E.D. Siggia, B.I. Halperin and P.C. Hohenberg, Phys. Rev. B 13 (1976) 2110.
[7] P.C. Hohenberg and B.I. Halperin, Rev. Modern Phys. 49 (1977) 435.
[8] R. Ruiz and D.R. Nelson, Phys. Rev. A 23 (1981) 3224.
[9] R. Ruiz and D.R. Nelson, Phys. Rev. A 24 (1981) 2727.
[10] A.N. Kolmogorov, C.R. Acad. Sci. USSR 30, 301; ibid 32 (1941) 16.
[11] A.M. Obukhov, Izv. Akad. Nauk. SSSR. Ser. Geogr. Geofiz. 13 (1949) 58.
[12] T. Bohr, M.H. Jensen, G. Paladin and A. Vulpiani, Dynamical Systems Approach to Turbulence (Cambridge University Press, Cambridge), to be published.
[13] R.S. Iroshnikov, Sov. Astron. 7 (1963) 566.
[14] R.H. Kraichnan, Phys. Fluids 8 (1965) 1385.
[15] A.M. Obukhov, Atmos. Oceanic. Phys. 7 (1971) 41.
[16] E.B. Gledzer, Sov. Phys. Dokl. 18 (1973) 216.
[17] V.N. Desnyansky and E.A. Novikov, Prinkl. Mat. Mekh. 38 (1974) 507.
[18] J. Eggers and S. Grossmann, Phys. Lett. A 156 (1991) 444; S. Grossmann and D. Lohse, Z. Phys. B 89 (1992) 11.
[19] E. Aurell, P. Frick and Shaidurov, Physica D 72 (1994) 95.
[20] M. Yamada and K. Ohkitani, J. Phys. Soc. Japan 56 (1987) 4210; Prog. Theoret. Phys. 79 (1988) 1265.
[21] M.H. Jensen, G. Paladin and A. Vulpiani, Phys. Rev. A 43 (1991) 798.
[22] L. Kadanoff, D. Lohse, J. Wang and R. Benzi, Phys. Fluids 7 (1995) 617; L. Kadanoff, Phys. Today 48 (1995) 11.
[23] R. Benzi, L. Biferale and G. Parisi, Physica D 65 (1993) 163.
[24] L. Biferale, A. Lambert, R. Lima and G. Paladin, Physica D 80 (1995) 105.
[25] A. Brandenburg, K. Enqvist and P. Olesen, Phys. Rev. D 54 (1996) 1291.
[26] G. Parisi, preprint unpublished of the University of Rome (1990).
[27] L. Biferale and R. Kerr, Phys. Rev. E 52 (1995) 6113.
[28] M.H. Jensen, G. Paladin and A. Vulpiani, Phys. Rev. A 45 (1992) 7214.
[29] W. Heisenberg, Proc. Roy. Soc. Sub. A 195 (1948) 402.
[30] U. Frisch, Turbulence: The Legacy of A.N. Kolmogorov (Cambridge University Press, Cambridge, 1995).
[31] T. von Karman and L. Howarth, Proc. Roy. Soc. Ser. A 164 (1938) 192.
[32] A. Brandenburg, K. Enqvist and P. Olesen, Phys. Lett. B 392 (1997) 395.
[33] A. Pouquet, U. Frisch and J. Léorat, J. Fluid Mech. 77 (1976) 321.
[34] D. Biskamp, Phys. Rev. E 50 (1994) 2702.
[35] K. Kumar, S. Fauve and O. Thual, J. de Physique II 6 (1996) 945.